Evidence for Molecular Translational Diffusion during the Crystallization of Amorphous Solid Water

R. Scott Smith, C. Huang, and Bruce D. Kay*

Environmental Molecular Sciences Laboratory, Pacific Northwest National Laboratory, P.O. Box 999, Mail Stop K2-14, Richland, Washington 99352

Received: October 11, 1996; In Final Form: April 23, 1997[⊗]

Molecular diffusion in amorphous solid water is studied by measuring the extent of isotope exchange and mixing in vapor-deposited ultrathin films using temperature-programmed desorption. Our results indicate there is long-range translational diffusion that occurs concomitantly with the amorphous to crystalline ice phase transition. The apparent diffusivity estimated from these data is a factor of $10^{6\pm1}$ greater than an Arrhenius extrapolation for diffusion in crystalline ice. This finding suggests that the amorphous material exhibits liquid-like translational diffusion prior to crystallization at temperatures near 155 K.

Introduction

The physical and structural properties of amorphous solid water (ASW) have been the subject of numerous publications and are summarized in recent reviews.[1−3] One reason for the interest is the idea that ASW could be used to understand the behavior of liquid water. Despite this prospect, a question remains as to whether ASW is a metastable extension of normal supercooled water or a distinct phase.[4−13] The uncertainty on the nature of ASW arises from the following arguments. The first involves a debate over whether a thermodynamic continuity of state can exist between ASW and supercooled water.[9−11,13,14] Theoretical estimates of the free energy do not allow the amorphous solid water to be connected with normal liquid water by a reversible thermodynamic path. Additionally, the measured thermodynamic and transport properties of supercooled liquid water are well described by a power law equation which has a singularity at 228 K (−45 °C).[2,4,12,15] Such a singularity would preclude a connection between ASW and the supercooled liquid.

Water vapor deposited on low-temperature substrates (<145 K) is known to form an amorphous phase termed ASW that is metastable with respect to crystalline ice.[1] ASW has a higher free energy than crystalline ice and as a result has a higher vapor pressure and desorption rate.[13,16,17] Previously, we used quantitative temperature-programmed desorption (TPD) to accurately determine the relative free energy between the two phases near 150 K,[13] thereby demonstrating that a reversible thermodynamic path between ASW and supercooled liquid water is possible. Recently we have also used the difference in desorption rates between ASW and crystalline ice to study the kinetics of crystallization.[19]

There is still debate about whether ASW becomes a liquid before it freezes to ice near 150 K. From spectroscopic studies of the rates of isotope exchange in ASW, Fisher and Devlin[18] conclude that the very weak calorimetric glass transition reported[11,19,20] near 130 K is a manifestation of the onset of molecular rotation in the glass rather than the transformation to a diffusing liquid and that ASW freezes directly to crystalline ice near 150 K without passing through an intermediate liquid state.

In an effort to examine the nature of the molecular motion accompanying crystallization, we employ molecular beams with high spatial resolution to create ultrathin (<5000 Å) films of roughly equivalent thicknesses of either solid amorphous H_2O and D_2O, or $H_2{}^{16}O$ and $H_2{}^{18}O$. TPD is used to study the extent of reaction and mixing of the layered interfaces. The desorption spectra reveal the details of the molecular diffusion length scales and are used to estimate the molecular diffusivity. Our results indicate there is long-range translational diffusion that occurs concomitantly with the amorphous to crystalline ice phase transition. The apparent diffusivity estimated from these data is a factor of $10^{6\pm1}$ greater than an Arrhenius extrapolation for diffusion in crystalline ice. This finding suggests that the amorphous material exhibits liquid-like translational diffusion prior to crystallization at temperatures near 155 K.

Experimental Section

The experimental technique and apparatus have been described elsewhere and are only summarized here.[21,22] In brief, a quadruply differentially-pumped effusive molecular beam of H_2O (D_2O, $H_2{}^{18}O$) was used to dose the single-crystal substrates. This highly collimated beam has a circular profile of ∼0.35 cm diameter and enables precise and reproducible exposures to be attained without appreciable adsorption on surfaces other than the sample crystals. A flux of 0.06 ML/s (ML = 10^{15} molecules/cm^2) was used to grow precise thicknesses of ASW films on the single-crystal substrates at 85 K. Both Au(111) and Ru(001) single crystals were used as substrates for film deposition, and the results were independent of the substrate. These substrates were prepared, cleaned, and ordered using standard techniques.[21,22] Films of varying composition were prepared by sequential dosing of the isotopic vapor. After ASW film growth, the substrates were resistively heated at a ramp rate of 0.6 K/s from 85 K to a temperature above which the ice film had completely desorbed. A quadrupole mass spectrometer was used to measure the angle-integrated desorption rate as a function of time. The mass spectrometer signals are corrected for mass fragmentation effects that occur during electron impact ionization and are converted to absolute desorption rates in ML/s.

Results and Discussion

Figure 1A displays TPD spectra for amorphous deposits of H_2O and D_2O grown in a side-by-side configuration. Each isotopic column is grown to a nominal height of 33 ML, and the column centers are separated by 0.50 cm. The desorption

* Author to whom correspondence should be addressed.
[⊗] Abstract published in *Advance ACS Abstracts,* June 15, 1997.

S1089-5647(96)03278-6 CCC: $14.00

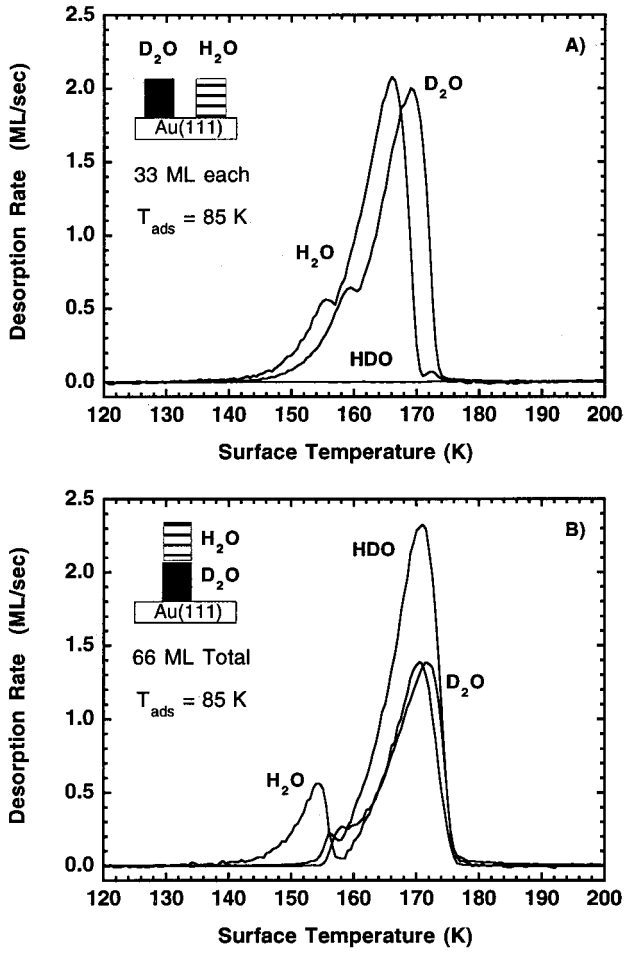

Figure 1. (A) TPD spectra for amorphous deposits of H_2O (33 ML) and D_2O (33 ML) grown in a side-by-side configuration. (B) TPD spectra for amorphous deposits of H_2O (33 ML) grown on top of D_2O (33 ML) for a total thickness of 66 ML.

spectra for H_2O and D_2O are similar but are shifted by about 5 K. This shift is due to zero-point energy differences between H_2O and D_2O.[1] Both the H_2O and D_2O deposits show a "bump" in their desorption spectra at ~154 and 160 K respectively. This feature arises from the irreversible amorphous to crystalline phase transformation. The amorphous deposits crystallize to cubic ice I in the 155−170 K range.[11,13,19,20,23−27] The desorption rate from the amorphous phase is greater than from the crystalline phase because of the excess free energy of the metastable phase. The bump is observed during the transformation to the more stable crystalline phase. Quantitative measurements of the desorption rates from the amorphous and crystalline phases of H_2O and D_2O have been reported previously.[13] The kinetics of the crystallization are discussed in detail elsewhere,[27] but for the purpose of this study the bump in the TPD spectrum is the hallmark of crystallization.

Figure 1A also illustrates the high spatial resolution of the molecular beam dosing technique. The lack of HDO formation indicates that the deposits are grown and desorb without intermixing of the two columns. It is important to note that the diameter of these deposits is approximately 0.35 cm while the height is about 100 Å. This geometry has about 10^5 times more surface area on the top than on the column sides, and as such, the desorption is essentially one-dimensional. The drawings on the figures schematically represent the initial relative positions of the various water isotopes within the film.

Figure 1B displays TPD spectra for an amorphous film of H_2O (~33 ML) grown on top of D_2O (~33 ML). Below 154 K, only H_2O (the species on top) desorbs. At higher temperatures, H_2O, D_2O, and HDO are all detected. The HDO and D_2O signals rise abruptly at a temperature near the onset of the phase transition in concert with a precipitous decrease in the H_2O signal. The HDO signal results from isotopic exchange between the H_2O and D_2O and provides clear evidence for the mass transport of hydrogen isotopes within the film. The TPD spectra show that prior to the phase transition the isotopically labeled ices have not mixed, but after the phase transition complete mixing is observed. The evidence for complete mixing is the 1:2:1 (H_2O:HDO:D_2O) ratio of the signal intensities. This ratio is expected for complete statistical scrambling of equal amounts of H_2O and D_2O. In this experiment long-range mixing of hydrogen isotopes has occurred over the entire length of the 66 ML thick film, approximately 200 Å. Analogous results are obtained when D_2O films are grown on top of H_2O films except that D_2O desorption occurs first.

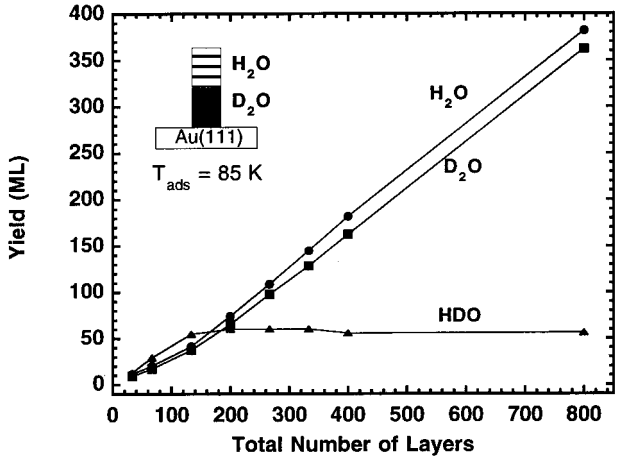

Figure 2. Integrated product yields for H_2O, D_2O, and HDO formed during the TPD of equal amounts of H_2O grown on top of D_2O for various total initial thicknesses.

The above results suggest that diffusion is occurring in concert with the phase transition. To determine the length scale over which hydrogen isotope exchange occurs during crystallization, experiments analogous to those displayed in Figure 1B were performed for various initial film thicknesses. The ASW films were prepared with an approximately equal number of H_2O and D_2O layers. The results of these experiments as a function of total film thickness are displayed in Figure 2. The H_2O, D_2O, and HDO TPD spectra are integrated to determine the absolute yield of the various isotopic products. These isotopic product yields are plotted as a function of the initial total thickness of amorphous film. The finite length scale of diffusion is evident from the amount of the HDO isotope exchange product. Initially the yield of HDO product increases with total film thickness but levels off at a saturation value as the initial film thickness increases. The saturation in the HDO product yield occurs for films thicker than about 100 ML and is suggestive of a mixing zone extending approximately 300 Å in length. Diffusive motion is "frozen" by the crystal structure after the crystallization is complete. The diffusion length must therefore be limited by the finite time needed for complete crystallization. When the film is thick compared to the diffusion length possible in this finite time, complete mixing does not occur.

The H/D isotope exchange kinetics alone cannot definitively indicate whether there is large scale "molecular" translational motion because of the possibility of a tunneling and/or rotation hydrogen exchange mechanism. In an effort to further characterize the mass transport mechanism, we have used $H_2{}^{16}O$ and $H_2{}^{18}O$ labeled water in our isotopic mixing experiments.

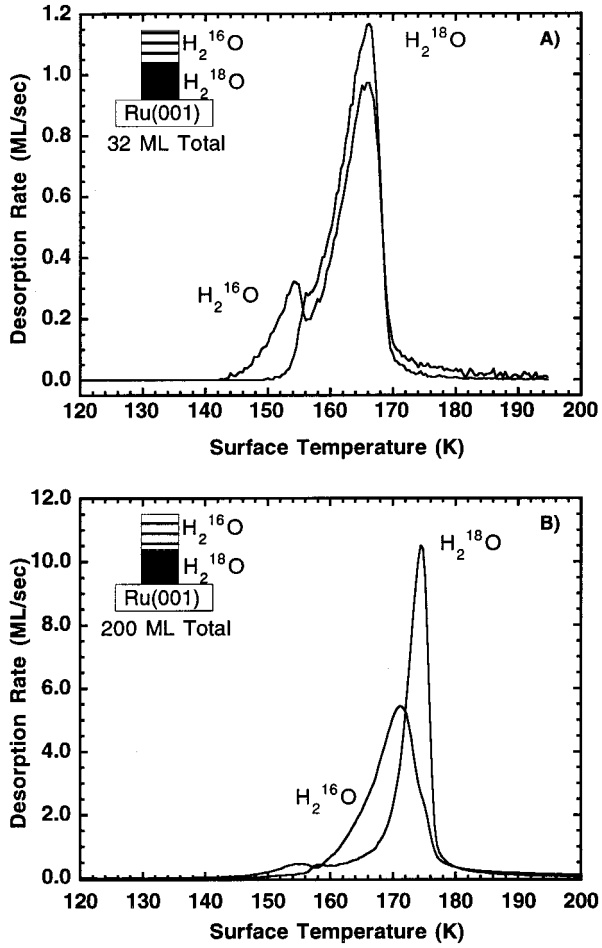

Figure 3. (A) TPD spectra for amorphous deposits of $H_2{}^{16}O$ (16 ML) grown on top of $H_2{}^{18}O$ (16 ML) for a total thickness of 32 ML. (B) TPD spectra for amorphous deposits of $H_2{}^{16}O$ (100 ML) grown on top of $H_2{}^{18}O$ (100 ML) for a total thickness of 200 ML.

Figure 3A shows the TPD spectra for films of 16 ML of $H_2{}^{16}O$ grown on top of 16 ML of $H_2{}^{18}O$ ASW. The spectra show that prior to the phase transition the isotopically labeled ices have not mixed, but after the phase transition, complete mixing is observed. Note that the onset of isotopic mixing is abrupt and occurs concomitant with the phase transformation of ASW into crystalline ice. Figure 3B shows that for thicker films, 200 ML total in this experiment, only a finite amount of mixing has occurred during the time scale of the phase transition. Analogous results are obtained when the isotope dose order is reversed. Analysis of numerous TPD spectra indicates that $H_2{}^{16}O$ and $H_2{}^{18}O$ mixing occurs over similar length scales as the H/D exchange. These experimental observations demonstrate that the observed isotopic mixing results from molecular translational diffusion.

The above data suggest that long-range translational diffusion occurs in concert with the crystallization of amorphous ice. Two other possibilities that could potentially give rise to apparent long-range intermixing are roughening of the interface during desorption and crack or grain formation concomitant with the phase transition. Both of these processes will lead to exposure of the underlying layers prior to desorption of the outermost layer. While these processes probably both occur to some extent, we do not believe they are responsible for the observed intermixing for the following reasons. In the absence of lateral diffusion, statistical fluctuations in both adsorption and desorption will give rise to a surface roughness having a bandwidth equivalent to the square root of the number of layers. Lateral diffusion will result in even less roughness. As displayed in Figure 2, we observe complete intermixing for films below 100 layers thick. Furthermore, we observe complete H/D isotope exchange within the intermixed region. Clearly, such exchange requires intimate chemical contact between the isotopes. Such contact is not expected for desorption from exposed lower layers or release of the underlying layers via cracks or grain boundaries.

Summary

Our results clearly indicate that molecular translational diffusion occurs at a measurable rate within these ASW films. We find complete isotopic scrambling over distances up to 300 Å at temperatures as low as 155 K. As evidenced by the abrupt onset of isotopic mixing and exchange, translational diffusion appears to occur concomitantly with crystallization over the narrow temperature range (~6 K) of the amorphous to crystalline phase transition observed in the TPD experiments. At the heating rates employed in these experiments, this temperature range corresponds to a time scale of about 10 s. An order of magnitude estimate of the translational diffusivity, D, can be obtained using the relation $D = L^2/t$, where L is the diffusion length and t is time. Our data give an apparent diffusivity of approximately $10^{-12\pm1}$ cm^2/s. Diffusion measurements in ice have been reported for temperatures from 273 to 233 K.[28,29] Arrhenius extrapolation of these measurements to 160 K predicts a crystalline diffusivity below 10^{-18} cm^2/s. Such a diffusivity would result in motion of less than 1 ML on the time scale of our TPD experiment.

Despite the approximate nature of our estimate, the experimental results cannot be explained by the diffusivity for crystalline ice. The apparent diffusivity in ASW estimated from the experimental data is a factor of $10^{6\pm1}$ greater than an Arrhenius extrapolation for diffusion in crystalline ice. This finding suggests that the amorphous material exhibits liquid-like translational diffusion prior to crystallization at temperatures near 155 K. Thus the observed diffusive behavior may be more consistent with that of a liquid (albeit a very viscous liquid) than a solid. A diffusivity of $10^{-12\pm1}$ cm^2/s for ASW near 155 K would imply a viscosity $10^{7\pm1}$ times greater than that of liquid water at 300 K. Current efforts in our laboratory are focused on determining the temperature dependence of the ASW diffusivity. Knowledge of the temperature dependence is requisite to determine if the diffusivity of ASW can be connected to the transport properties of normal and supercooled liquid water.

Acknowledgment. This work is supported by the U.S. Department of Energy Office of Basic Energy Sciences, Chemical Sciences Division. Pacific Northwest National Laboratory is operated for the U.S. Department of Energy by Battelle under Contract DE-AC06-76RLO 1830.

References and Notes

(1) Sceats, M. G.; Rice, S. A. Amorphous water and its relationship to liquid water: A random network model for water. In *Water A Comprehensive Treatise*, 1st ed.; Franks, F., Ed.; Plenum Press: New York, 1982; Vol. 7; p 83.
(2) Angell, C. A. *Annu. Rev. Phys. Chem.* **1983**, *34*, 593.
(3) Angell, C. A. *Science* **1995**, *267*, 1924.
(4) Speedy, R. J.; Angell, C. A. *J. Chem. Phys.* **1976**, *65*, 851.
(5) Maddox, J. *Nature* **1987**, *326*, 823.
(6) Prielmeier, F. X.; Lang, E. W.; Speedy, R. J.; Ludemann, H.-D. *Phys. Rev. Lett.* **1987**, *59*, 1128.
(7) Angell, C. A. *Nature* **1988**, *331*, 206.
(8) Sorensen, C. M. *Nature* **1992**, *360*, 303.
(9) Speedy, R. J. *J. Phys. Chem.* **1992**, *96*, 2322.
(10) Johari, G. P. *J. Chem. Phys.* **1993**, *98*, 7324.
(11) Johari, G. P.; Fleissner, G.; Hallbrucker, A.; Mayer, E. *J. Phys. Chem.* **1994**, *98*, 4719.

(12) Debenedetti, P. G. In *Physical Chemistry of Aqueous Systems: Meeting the Needs of Industry*; Proceedings of the 12th International Conferences of Water & Steam; White, H. J., Sengers, J. V., Neumann, D. B., Bellows, J. C., Eds.; Begell House: New York, 1995; p 339.
(13) Speedy, R. J.; Debenedetti, P. G.; Smith, R. S.; Huang, C.; Kay, B. D. *J. Chem. Phys*. **1996**.
(14) Johari, G. P. *Philos. Mag*. **1977**, *35*, 1077.
(15) Angell, C. A. Supercooled Water. In *Water A Comprehensive Treatise*, 1st ed.; Franks, F., Ed.; Plenum Press: New York, 1982; Vol. 7, Chapter 1.
(16) Kouchi, A. *Nature* **1987**, *330*, 550.
(17) Sack, N. J.; Baragiola, R. A. *Phys. Rev. B* **1993**, *48*, 9973.
(18) Fisher, M.; Devlin, J. P. *J. Phys. Chem*. **1995**, *99*, 11584.
(19) Hallbrucker, A.; Mayer, E.; Johari, G. P. *J. Phys. Chem*. **1989**, *93*, 4986.
(20) Handa, Y. P.; Klug, D. D. *J. Phys. Chem*. **1988**, *92*, 3323.
(21) Kay, B. D.; Lykke, K. R.; Creighton, J. R.; Ward, S. J. *J. Chem. Phys*. **1989**, *91*, 5120.
(22) Brown, D. E.; George, S. M.; Huang, C.; Wong, E. K. L.; Rider, K. B.; Smith, R. S.; Kay, B. D. *J. Phys. Chem*. **1996**, *100*, 4988.
(23) Sugasaki, M.; Suga, H.; Seki, S. *Bull. Chem. Soc. Jpn*. **1968**, *41*, 2591.
(24) Handa, Y. P.; Klug, D. D.; Whalley, E. *J. Chem. Phys*. **1986**, *84*, 7009.
(25) Floriano, M. A.; Handa, Y. P.; Klug, D. D.; Whalley, E. *J. Chem. Phys.* **1989**, *91*, 7187.
(26) Jenniskens, P.; Blake, D. F. *Science* **1994**, *265*, 753.
(27) Smith, R. S.; Huang, C.; Wong, E. K. L.; Kay, B. D. *Surf. Sci. Lett*. **1996**, *367*, L13.
(28) Onsager, L.; Runnels, L. K. *J. Chem. Phys*. **1969**, *50*, 1089.
(29) Goto, K.; Hondoh, T.; Higashi, A. *Jpn. J. Appl. Phys*. **1986**, *25*, 351.